activation of intracellular signaling cascades, including those of NF-κB, STAT3, and MAPK. Additionally, ErbB1 and its ligands have been shown to influence cellular growth and proliferation and are mainly associated with cancers and neoplasm processes. We recently showed that the epiregulin/ErbB1 axis contributes to activation of the inflammation amplifier and subsequent chronic inflammation development via the PI3Kα/NF-κB pathway. Furthermore, blocking the epiregulin/ErBb1 pathway suppresses several inflammatory disease models, whereas serum concentrations of epiregulin are higher in patients with inflammatory disease (4). In the present study, we investigated the relationship between other growth factors and local chemokine and IL-6 expression via the inflammation amplifier during the development of inflammation, mainly in an animal model of rheumatoid arthritis (RA).

In this study, we showed that the serum concentrations of several growth factors were increased in RA patients, whereas local blockades of each growth factor suppressed the development of cytokine-induced arthritis in mice by suppressing chemokine and IL-6 expressions. To understand why these growth factors act independently during the development of inflammation, we examined their temporal expression in joints. Only epiregulin was expressed by cytokine-mediated NF-κB and STAT3 activation. Epiregulin directly triggered the expression of other growth factors, although at the same time its expression was dependent on these growth factors at later time points of arthritis development. Consistent with this result, synovial cells expressed epiregulin by day 1 after cytokine injection, whereas the expression of other growth factors was observed at later times. Furthermore, elevated levels of various growth factors were detected in sera of patients suffering from multiple sclerosis (MS). Affected spinal cords in an MS model, experimental autoimmune encephalomyelitis (EAE), expressed most of the growth factors, and EAE symptoms were suppressed by the blockade of TGF-α. These results suggest that the temporal expression of growth factors triggered by the cytokine/epiregulin axis is independently involved in the development of various inflammatory diseases. Therefore, each growth factor pathway might be an independent therapeutic target for many inflammatory diseases, including RA and MS.

Materials and Methods

Human serum preparations

Serum was collected from 11 patients with RA at Tokyo Medical and Dental University Hospital and from 21 patients with clinically defined MS (negative for autoantibody presence) at Osaka University Hospital. Serum was also collected from 41 healthy subjects at Osaka University Health Care Center. Informed consent was obtained from each subject. This study was approved by the Ethics Committees of Osaka University Hospital and Tokyo Medical and Dental University. Serum levels of Areg, BTC, TGF-α, FGF2, PLGF, and tenascin C (TNC) in patients were measured by a Milliplex kit (Merck, Tokyo, Japan) followed by analysis with a multiplex analysis device (Bio-Rad Laboratories, Tokyo, Japan).

Mouse strains

C57BL/6 and DBA/1J mice were purchased from Japan CLEA (Tokyo, Japan) or Japan SLC (Shizuoka, Japan). F759 mice, which carry a human gp130 variant (S710L), were backcrossed with C57BL/6 mice for >10 generations (8). NF-κB reporter transgenic mice in a C57BL/6 background were backcrossed with F759 mice and used for experiments (9). All mice were maintained under specific pathogen-free conditions according to the protocols of the Osaka University Medical School. All animal experiments were performed following the guidelines of the Institutional Animal Care and Use Committees of the Graduate School of Frontier Biosciences and the Graduate School of Medicine, Osaka University.

Abs and reagents

The following Abs were used for in vivo neutralization and immunohistochemistry: monoclonal anti-mouse Areg Ab, anti-mouse BTC Ab, anti-mouse epiregulin Ab, anti-human TGF-α Ab, anti-mouse PLGF2 Ab, anti-human/mouse TNC Ab (R&D Systems, Minneapolis, MN), anti-mouse FGF2 Ab (Millipore, Tokyo, Japan), polyclonal anti-mouse epiregulin Ab (Santa Cruz Biotechnology, Santa Cruz, CA), anti-mouse FGF2 Ab (Abcam, Tokyo, Japan), and purified rat IgG (Sigma-Aldrich, Tokyo, Japan). The following Abs were used for Western blotting: anti–phospho-p65 (Ser^{536}, 93H1), anti–phospho-Akt (Ser^{473}, 193H12), anti-Akt (all from Cell Signaling Technology, Tokyo, Japan), anti-p65 (C-20) (Santa Cruz Biotechnology), anti–α-tubulin (Sigma-Aldrich), HRP-conjugated goat anti-rabbit IgG (H+L) (SouthernBiotech, Birmingham, AL), and HRP-conjugated goat anti-mouse IgG (H+L) (Invitrogen, Carlsbad, CA). The following Abs were used for flow cytometry analysis: allophycocyanin-conjugated anti–IFN-γ (eBioscience, San Diego, CA) and control IgG1κ (eBioscience); FITC-conjugated anti-CD8 (eBioscience), anti-CD11b (Beckman Coulter, Brea, CA), anti-CD11c (eBioscience), anti-CD19 (eBioscience), anti-NK1.1 (eBioscience), and anti–I-A/I-E (BioLegend, Tokyo, Japan); PE-conjugated anti–IL-17A (eBioscience), control IgG2a (eBioscience), and anti–I-A/I-E (BioLegend); and PE-Cy7–conjugated anti-CD4 (BioLegend).

Mission TRC short hairpin RNA (shRNA) clones, LPS, puromycin, polybrene, MOG_{33-55}, pertussis toxin, IFA, protease inhibitor mixture, phosphatase inhibitor mixture 2, phosphatase inhibitor mixture 3, and MTT (thiazolyl blue) were purchased from Sigma-Aldrich. Mouse Areg, BTC, epiregulin, FGF2, PLGF2, IL-23, human TGF-α, TNC, and soluble IL-6Rα were purchased from R&D Systems. Mouse IL-17 was purchased from PeproTech (Rocky Hill, NJ). Human IL-6 was purchased from Toray Industries (Tokyo, Japan). LY294002 was purchased from Merck.

Intra-articular injections (joint injections)

IL-17A (R&D Systems), IL-6 (Toray Industries), or saline were injected into the joints as described previously (10). Joints were injected with lentivirus carrying shRNA specific for Areg, BTC, Tgfa, Fgf2, Plgf2, TNC, and NF-κB p65 (RelA) (Sigma-Aldrich) or with a lentivirus carrying a scrambled sequence (Sigma-Aldrich) or anti-Areg, anti-BTC, anti–TGF-α, anti-FGF2, anti-PLGF2, and anti-TNC Abs.

Real-time PCRs

Total RNA was prepared from BC1 and MEF cells using a GenElute mammalian total RNA kit (Sigma-Aldrich) or prepared from synovial tissues of mouse knee joints using Sepasol-RNA I (Nacalai Tesque, Kyoto, Japan), chloroform (Sigma-Aldrich), and isopropanol (Sigma-Aldrich). The RNA was then treated with DNase I (Sigma-Aldrich) and used for reverse transcription with Moloney murine leukemia virus reverse transcriptase (Promega, Tokyo, Japan). cDNA product was used in each real-time PCR reaction. A 7300 Fast real-time PCR system (Applied Biosystems, Tokyo, Japan) and SYBR Green PCR master mix (Kapa Biosystems, Woburn, MA) were used to quantify levels of target mRNA and hypoxanthine phosphoribosyltransferase (HPRT) mRNA. The PCR primer pairs were as follows (forward/revers): mouse HPRT primers, 5′-GATTAGCGATGATGAACCAGGTT-3′ and 5′-CCTCCCATCTCCTTCATGACA-3′; mouse IL-6 primers, 5′-GAGGATACCACTCCCAACAGACC-3′ and 5′-AAGTGCATCATCGTTGTTCATACA-3′; mouse CCL20 primers, 5′-CGACTGTTGCCTCTCGTACA-3′ and 5′-GAGGAGGTTCACAGCCCTTT-3′; mouse epiregulin primers, 5′-CTGCCTCTTGGGTCTTGACG-3′ and 5′-GCGGTACAGTTATCCTCGGATTC-3′; mouse Areg primers, 5′-GCAGATACATCGAGAACCTGG-3′ and 5′-CTGCAATCTTGGATAGGTCCTTG-3′; mouse BTC primers, 5′-AATTCTCCACTGTGTGGTAGCA-3′ and 5′-GGTTTTCACTTTCTGTCTAGGGG-3′; mouse TGF-α primers, 5′C-ACTCTGGGTACGTGGGTG-3′ and 5′-CACAGGTGATAATGAGGACAGC-3′; mouse FGF2 primers, 5′-GAGTTGTGTCTATCAAGGGAGTG-3′ and 5′-CCGTCCATCTTCCTTCATAGC-3′; mouse PLGF2 primers, 5′-TCTGCTGGGAACAACTCAACA-3′ and 5′-GTGAGACACCTCATCAGGGTAT-3′; mouse TNC primers, 5′-CACAACCCGTGAGTACCAGC-3′ and 5′-AGAGGGTATGCTATAAGCCAGAA-3′; mouse E-cadherin primers, 5′-CCAATCCTGATGAAATTGGAAACT-3′ and 5′-CGTAATCGAACACCAACAGAGAGT-3′; and mouse β-actin primers, 5′-GGCTGTATTCCCCTCCATCG-3′ and 5′-CCAGTTGGTAACAATGCCATGT-3′. The conditions for real-time PCRs were 40 cycles at 94°C for 15 s followed by 40 cycles at 60°C for 60 s. The relative mRNA expression levels were normalized to the levels of HPRT mRNA.

For some experiments, the ankles were used because they provide an easier assessment of restricted mobility by inflammation than do knee joints. Quantitative PCR analysis was performed using knee tissues, because a larger amount of RNA can be obtained and there is no need to pool samples from several mice, which reduces the number of animals used. We confirmed that the quantitative PCR results were equivalent between ankle and knee samples.

Clinical assessment of arthritis

Mice were inspected and assessed for signs of arthritis as described previously (4, 8, 10). In brief, the severity of the arthritis was determined based on two bilaterally assessed parameters: 1) swelling in the ankle, and 2) restricted mobility of the ankle joints. The severity of each parameter was graded on a scale of 0–3: 0, no change; 1, mild change; 2, medium change; and 3, severe change. Averages for a single point in one leg ankle joint from each mouse were used. The disease phenotypes and the histology were scored blindly. In some experiments, we injected shRNA lentiviruses into the joints because we hypothesized that the shRNA lentiviruses would reduce target expressions due to their significant knockdown of genes in BC1 cells.

Cells and stimulation conditions

A type 1 collagen$^+$ endothelial cell line of BC1 cells was obtained from Dr. M. Miyasaka (Osaka University) (4). For stimulation, BC1 cells were plated in 96-well plates (1×10^4 cells/well) and stimulated with human IL-6 (50 ng/ml; Toray Industries) plus human soluble IL-6R (50 ng/ml; R&D Systems) and/or mouse IL-17A (50 ng/ml; R&D Systems) for 3 or 24 h after 2 h of serum starvation. Cell culture supernatant was collected for ELISA and cell growth was assessed by MTT assay. In some experiments, cells were harvested and total RNA was prepared for real-time PCRs.

ELISA

IL-6 concentrations in cell culture supernatant or serum were determined using ELISA kits (BD Biosciences).

MTT assay

Cell growth was determined with thiazolyl blue tetrazolium bromide (Sigma-Aldrich) according to the manufacturer's instructions.

Western blotting

BC1 cells were stimulated by the indicated cytokines and lysed with lysis buffer (20 mM Tris-HCl [pH 7.4], 150 mM NaCl, 1% Triton X-100, and 1 mM EDTA) supplemented with protease inhibitor mixture, phosphatase inhibitor mixture 2 (Sigma-Aldrich), and phosphatase inhibitor mixture 3 (Sigma-Aldrich). Twenty micrograms total protein was run on 5–20% SDS-PAGE (Wako, Tokyo, Japan). After transfer to a polyvinylidene fluoride membrane (Millipore), immunoblotting was performed according to the manufacturer's protocol.

Luciferase reporter assay

Ankle joints from NF-κB-reporter Tg/F759 mice were collected, and synovial tissues were homogenized in passive lysis buffer (Promega). After centrifugation, the supernatants were collected, and total protein amount was adjusted by the Bradford method. Luciferase activities of tissue lysates were measured using a luciferase reporter assay system (Promega).

Histological analysis

Ankle joints were fixed in 4% paraformaldehyde, decalcified for 12 h in Morse's solution (22.5% bornyl formate and 10% sodium acid citrate solution) followed by 12 h in 4% paraformaldehyde, and embedded in paraffin. Sections were stained with hematoxylin, anti–phospho-STAT3, anti–phospho-EGFR (Cell Signaling Technology), anti–phospho-p65, anti-vimentin (Sigma-Aldrich), anti–type 1 collagen (Abcam), anti-Areg, anti-FGF2 Ab, anti–TGF-α Ab, and anti-epiregulin Ab (10).

Passive transfer of pathogenic CD4$^+$ T cells from mice to induce EAE

EAE induction was performed as described previously (5, 11). Briefly, C57BL/6 mice or C57BL/6-PL mice were injected with a MOG_{35-55} peptide (Sigma-Aldrich) in CFA (Sigma-Aldrich) at the base of the tail on day 0 followed by i.v. injection of pertussis toxin (Sigma-Aldrich) on days 0, 2, and 7. On day 9, CD4$^+$ T cells from the resulting mice were sorted using anti-CD4 microbeads (Miltenyi Biotec, Tokyo, Japan). The resulting CD4$^+$ T cell–enriched population (4×10^6 cells) was cocultured with rIL-23 (10 ng/ml; R&D Systems) in the presence of MOG peptide–pulsed irradiated splenocytes (1×10^7 cells) for 2 d. Cells (1.5×10^7 cells) were then injected i.v. into wild-type mice. Clinical scores were measured as described previously (5, 11).

Mononuclear cell isolation from spinal cords

Mononuclear cells were isolated from spinal cords after cardiac perfusion with PBS, as described previously (11).

Intracellular cytokine staining

The number of Th17 cells in vivo was determined as described (12). In brief, T cells from spinal cords were stimulated with PMA and ionomycin (Sigma-Aldrich) in the presence of GolgiPlug (BD Biosciences) for 6 h. Intracellular IL-17 and IFN-γ were labeled with anti–IL-17 and anti–IFN-γ Abs, respectively, after surface staining, fixation, and permeabilization.

Flow cytometry

For cell surface labeling, 10^6 cells were incubated with fluorescence-conjugated Abs for 30 min on ice. The cells then were analyzed with a CyAn flow cytometer (Beckman Coulter, Tokyo, Japan). The collected data were analyzed using FlowJo software (Tree Star, Ashland, OR).

Statistical analysis

Student *t* tests (two-tailed) and a Williams' test were used for statistical analyses of differences between two groups. One-way ANOVA with a Dunnett post hoc analysis was used for multiple comparisons. A Wilcoxon rank-sum test was used for the statistical analyses of serum growth factor levels in humans (Figs. 1A, 4A) and clinical scores of arthritis and EAE (Fig. 1C, 1D, Supplemental Fig. 4B). A p value <0.05 was considered statistically significant.

Results

Various growth factors were increased in patients with RA

We previously showed that sera from patients suffering from RA have higher concentrations of epiregulin than do sera from control subjects (4). Also higher were the growth factors Areg, BTC, TGF-α, PLGF, TNC, and FGF2 (Fig. 1A). IL-6 concentration was also increased in sera from RA patients, as reported previously (4). These results suggest that various growth factors are involved in the development of inflammation.

Various growth factor pathways are critical for the development of a mouse RA model, F759 arthritis

We next investigated whether growth factors contribute to the development of arthritis in an RA model, F759 mice, which show spontaneous development of an arthritis that resembles human RA. These mice express a mutant variant of the IL-6 signaling transducer gp130 (Y759F) and have an enhanced IL-6–mediated STAT3 pathway due to deficient SOCS3-mediated negative feedback (8, 13). As these mice age, they spontaneously develop an MHC class II–associated, IL-6–dependent joint disease (F759 arthritis) that resembles RA (8, 14). Direct intra-articular injections (joint injections) of IL-17A and IL-6 with a minimum modification of hematopoietic cells induced arthritis within 2 wk in a manner dependent on NF-κB and STAT3 in nonimmune cells (10).

Joint injections of IL-17A and IL-6 increased the expressions of Areg, BTC, TGF-α, PLGF2 (mouse PLGF), TNC, and FGF2, as well as IL-6 in the joints (Fig. 1B). It was reported that EGF sometimes suppresses E-cadherin to induce epithelial–mesenchymal transition (15). We found that samples with increased TGF-α expression after IL-17 and IL-6 stimulation suppressed the expression of E-cadherin and had comparable expressions of β-actin to a control sample without cytokine stimulation (Supplemental Fig. 1A). We also confirmed that some growth factors were increased in other RA models such as collagen-induced arthritis and collagen Ab–induced arthritis (Supplemental Fig. 1B, 1C).

Importantly, joint injections of Abs against these growth factors or lentiviruses that had corresponding shRNA suppressed the development of the cytokine-induced arthritis (Fig. 1C, 1D). Furthermore, blockades of each growth factor decreased the expressions of IL-6 and CCL20 (Fig. 1E, 1F), which are essential for the development of arthritis (4, 10). These results suggest that growth factor pathways are independently involved in the development of cytokine-induced arthritis in vivo.

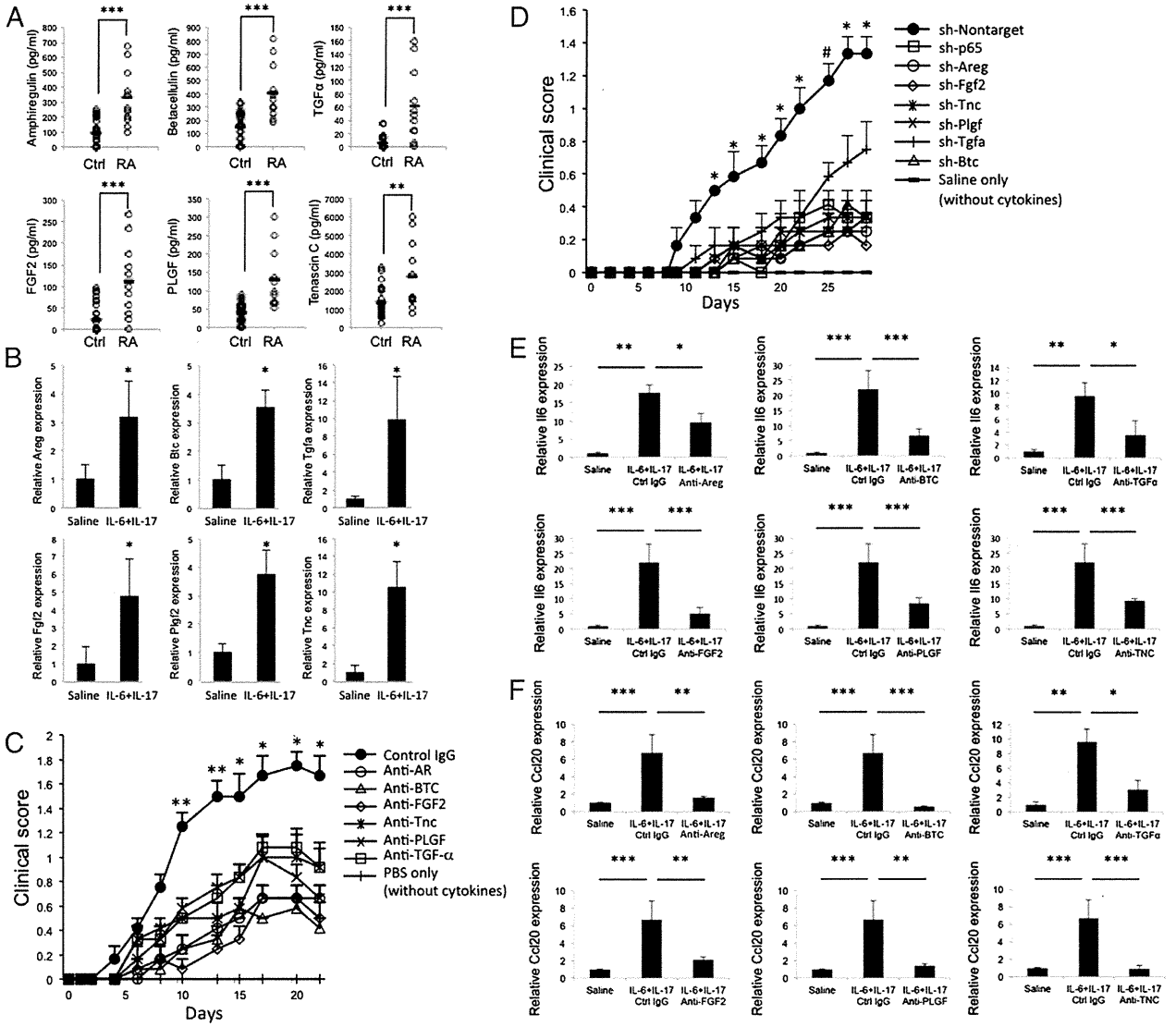

FIGURE 1. Areg, BTC, TGF-α, FGF2, PLGF, and TNC are critical for the development of cytokine-induced arthritis. (**A**) Serum concentrations of Areg, BTC, TGF-α, FGF2, PLGF, and TNC in patients suffering from RA (n = 11) compared with healthy age- and sex-matched subjects (n = 26). (**B**) IL-17A (0.2 μg) and IL-6 (0.2 μg) on days 0, 1, and 2 were injected into the knee joints of F759 mice. mRNA expressions of Areg, Btc, Tgfα, Fgf2, Plgf2, and TNC in joint synovial tissues were analyzed on day 7. (**C**) Clinical arthritis scores from the left legs of F759 mice after left ankle joint injections of 0.1 μg IL-6 and IL-17 on days 0, 1, and 2 and joint injections of anti-Areg Abs (1 μg, n = 6), anti-Btc Abs (1 μg, n = 6), anti–TGF-α Abs (1 μg, n = 6), anti-FGF2 Abs (1 μg, n = 6), anti-PLGF2 Abs (1 μg, n = 6), anti-TNC Abs (1 μg, n = 6), anti-IgG (1 μg, n = 6), or PBS with neither IL-6 nor IL-17 (n = 6) once every 2 or 3 d for 0–22 d. (**D**) Clinical arthritis scores from the left legs of F759 mice after left ankle joint injections of 0.1 μg IL-6 and IL-17 on days 6, 7, and 8 and joint injections of lentivirus encoding shRNA specific for p65 NF-κB (RelA) (1.9×10^5 transducing units [TU], n = 6), Areg (1.9×10^5 TU, n = 6), Btc (1.9×10^5 TU, n = 6), Tgfa (1.9×10^5 TU, n = 6), Fgf2 (1.9×10^5 TU, n = 6), Plgf2 (1.9×10^5 TU, n = 6), TNC (1.9×10^5 TU, n = 6), a nontarget sequence (1.9×10^5 TU, n = 6), or saline with neither IL-6 nor IL-17 (n = 6) on days 0, 2, and 4 during days 0–29. (**E** and **F**) IL-17 (0.2 μg) and IL-6 (0.2 μg) on days 0, 1, and 2 were injected into the knee joints of F759 mice in the presence or absence of joint injections of anti-Areg Ab (1 μg, n = 12), anti-BTC Ab (1 μg, n = 12), anti–TGF-α Ab (1 μg, n = 12), anti-FGF2 Ab (1 μg, n = 12), anti-Plgf2 (PLGF) Ab (1 μg, n = 12), anti-TNC Ab (1 μg, n = 12), or control IgG (1 μg, n = 12) on days 0, 1, 2, 4, and 6 followed by analysis of expressions of IL-6 (E) and CCL20 (F) in joint synovial tissues on day 7. Individual values, mean scores (A), and mean scores ± SEM (B–F) are shown. The p values were calculated using a Wilcoxon test (A, C, and D), Student t test (B), and one-way ANOVA (E and F). $*^{,\#}p < 0.05$, $**p < 0.01$, $***p < 0.001$; $*p < 0.05$ versus each treatment group in (C) and (D). $^{\#}p < 0.05$ versus sh-Fgf2, sh-Areg, sh-Btc, and sh-Plgf in (D).

Areg, BTC, TGF-α, and FGF2 play a role in the hyperexpression of IL-6 and chemokines via the PI3K/NF-κB pathway

We next identified which cell types produce and respond to growth factors in F759 arthritis. Immunohistochemistry experiments showed that >75% of observed cells had phosphorylated EGFR in the joints with cytokines and a similar percentage of cells had phosphorylated STAT3 and NF-κB and expressed various growth factors, including Areg, epiregulin, TGF-α, and FGF2 (Fig. 2A). Thus, cells that responded to EGF family growth factors were defined as type 1 collagen$^+$vimentin$^+$ synovial fibroblasts and concluded to synthesize growth factors.

To investigate how each growth factor enhances the expression of chemokines and IL-6, we employed the cell line BC1, because we have found a significant enhancement effect on IL-6 and chemokine expressions after stimulations of IL-17 and IL-6 in this line

(4, 5, 10, 16, 17). Chemokines and IL-6 expressions were significantly reduced in cultures without FBS, a rich source of growth factors, despite stimulation with IL-17A and/or IL-6 (Supplemental Fig. 2A) (4). We then obtained recombinant molecules of each growth factor. All except PLGF2 and TNC enhanced the expression of chemokines and IL-6 (Fig. 2B–D). These results suggest that the pathways of Areg, BTC, TGF-α, or FGF2 are directly involved in the enhanced expression of chemokines and IL-6, but those of PLGF2 and TNC are not.

It is important to understand how growth factors affect NF-κB and/or STAT3 signaling, and thus the inflammation amplifier. A PI3K inhibitor, LY294002, but not an MEK inhibitor, suppressed growth factor–mediated IL-6 expression (Fig. 2E, Supplemental Fig. 2B). Furthermore, Areg, BTC, TGF-α, and FGF2 enhanced the phosphorylation of Akt and p65 NF-κB in vitro and the activity of a NF-κB reporter in the presence of IL-17A and IL-6 in vivo (Fig. 2F, 2G). To confirm the importance of PI3K for growth factor–mediated IL-6 expression, we employed wortmannin and RNA interference. We used shRNA of PI3Kα because we previously reported epiregulin-EGFR enhances IL-6 expression via PI3Kα in the presence of IL-17 and IL-6 (4). Wortmannin and shRNA of PI3Kα suppressed growth factor–mediated IL-6 expression (Supplemental Fig. 2C, 2E), which demonstrates that PI3K, particularly PI3Kα, is critical for the growth factor–mediated en-

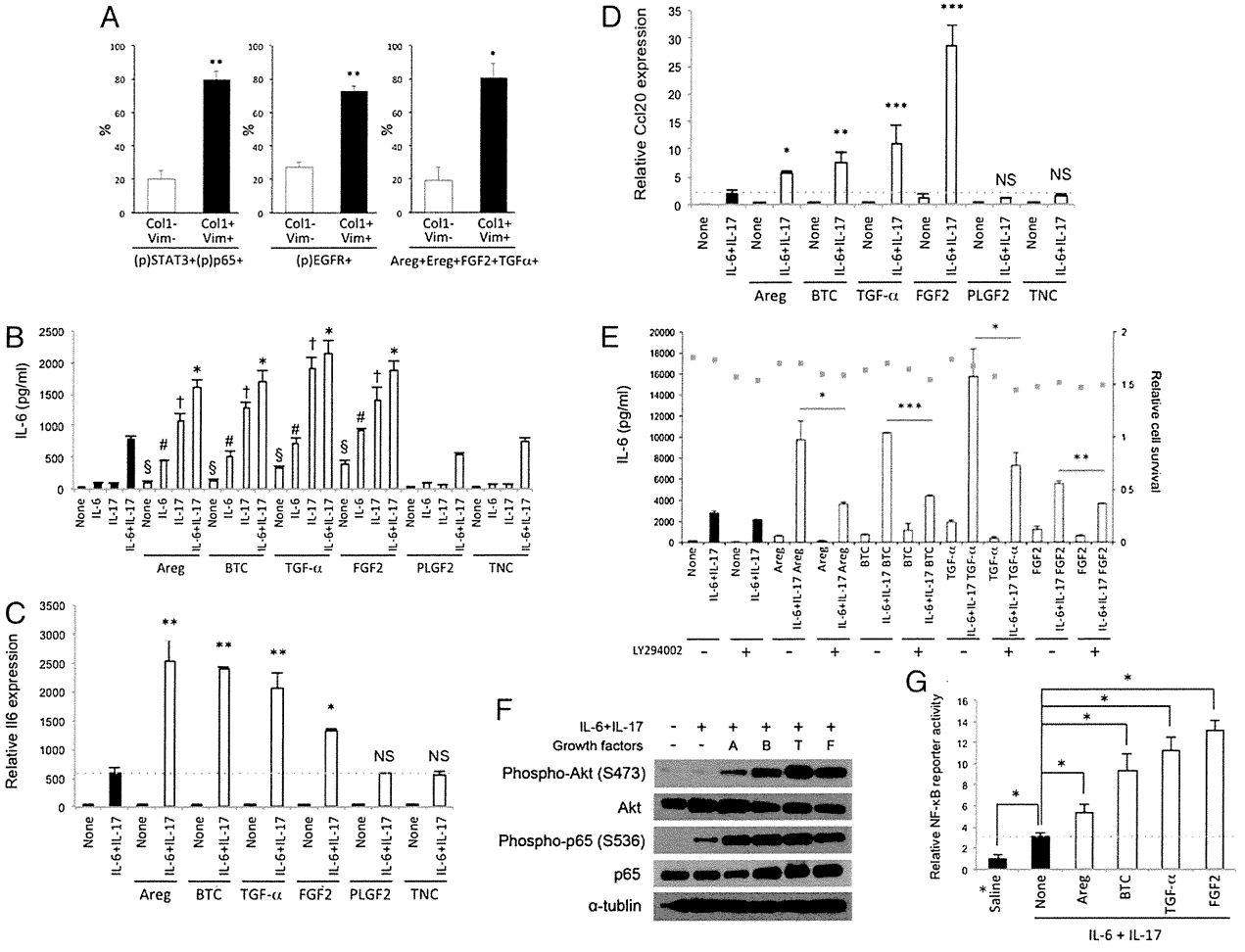

FIGURE 2. Areg, BTC, TGF-α, and FGF2 enhance the expressions of IL-6 and chemokines via the PI3K/NF-κB axis. (**A**) IL-6 (1 μg) and IL-17 (1 μg) were injected into the left ankle joints of F759 mice on days 0, 1, and 2. Immunohistochemistry of the left ankle joints was performed by using Abs against Areg, epiregulin (Ereg), FGF2, TGF-α, p-STAT3, p-p65, p-EGFR, type 1 collagen, and vimentin on day 7. These experiments were performed at least three times independently. Frequency of cells that showed activation of the inflammation amplifier (p-STAT3$^+$p-p65$^+$), received EGFR signaling (p-EGFR$^+$), or produced growth factors (Areg$^+$Ereg$^+$FGF2$^+$TGF-α$^+$) is indicated. Col1, type 1 collagen; Vim, vimentin. $*p < 0.05$, $**p < 0.01$ (Student t test). (**B**) BC1 cells were stimulated with human IL-6 plus soluble IL-6Rα and/or mouse IL-17 for 24 h with or without Areg, BTC, TGF-α, FGF2, PLGF2, and TNC. Culture supernatants were collected and assessed using ELISA specific for IL-6. Samples without growth factors (filled columns) were compared with samples with each growth factor. $^{\S}p < 0.05$, $*p < 0.01$, $^{\#,\dagger}p < 0.001$ (one-way ANOVA). (**C** and **D**) mRNA expressions of IL-6 (C) and CCL20 (D) in BC1 cells 3 h after stimulation with human IL-6 plus soluble IL-6Rα and mouse IL-17 with or without Areg, BTC, TGF-α, and FGF2 were evaluated using real-time PCR. Samples without growth factors (filled columns) were compared with samples with each growth factor. $*p < 0.05$, $**p < 0.01$, $***p < 0.001$ (one-way ANOVA). (**E**) BC1 cells were stimulated with human IL-6 plus soluble IL-6Rα in the presence or absence of Areg, BTC, TGF-α, or FGF2 for 24 h with or without 0.5 h pretreatment of LY294002 (3 μM) or DMSO vehicle control. Culture supernatants were collected and assessed using ELISA specific for mouse IL-6. Cell survival was evaluated based on mitochondrial activity. $*p < 0.05$, $**p < 0.01$, $***p < 0.001$ (Student t test). (**F**) BC1 cells were stimulated with human IL-6 plus soluble IL-6Rα and mouse IL-17 in the presence or absence of Areg (A), BTC (B), TGF-α (T), or FGF2 (F) for 30 min and then investigated for the phosphorylation of Akt and p65. (**G**) IL-6 and IL-17 were injected into the ankle joints of NF-κB reporter Tg/F759 mice with or without 0.2 μg Areg, BTC, TGF-α, or FGF2 followed by analysis of NF-κB reporter activity in the ankle joints on day 7 using the luciferase reporter assay system. $*p < 0.05$ (one-way ANOVA). Mean scores ± SD (A–E) and mean scores ± SEM (G) are shown.

hancement of inflammation. We also found that some growth factors enhance IL-6 expression in the presence of IL-17 and IL-6 in primary synovial fibroblasts in a manner dependent on PI3K (Supplemental Fig. 3A, 3B). Alternatively, PLGF2 and TNC increased cellular proliferation (Supplemental Fig. 3C). These results strongly suggest that most of the examined growth factors enhanced the PI3K/NF-κB pathway to increase the expression of chemokines and IL-6, whereas the roles of PLGF2 and TNC might locally increase cell growth to increase the number of cells involved in inflammation at diseased sites such as the joints.

Growth factor expressions are regulated in an epiregulin-triggered temporal manner

We next investigated why the growth factors act independently and with no compensation mechanisms for the development of cytokine-induced arthritis. IL-17A and IL-6, which are the triggering cytokines for inflammation development, increased epiregulin, but not the expression of the other growth factors in vitro (Fig. 3A). At the same time, epiregulin induced the expression of the other growth factors (Fig. 3B), probably after the development of inflammation. Consistent with this thought, joint injections of IL-17A and IL-6, which induce arthritis, increased epiregulin rapidly and intensely compared with other growth factors (Fig. 3C). Furthermore, the expressions of the other growth factors were suppressed in the presence of an epiregulin-neutralizing Ab even after joint injections of IL-17A and IL-6 (Fig. 3D, Supplemental Fig. 4A). Alternatively, blockade of each growth factor also suppressed epiregulin expression at later time points of the arthritis development (Fig. 3E), suggesting a reciprocal regulation mechanism between growth factors for the maintenance of epiregulin.

That epiregulin triggers a temporal expression of growth factors was also confirmed by immunohistochemistry. The expression of

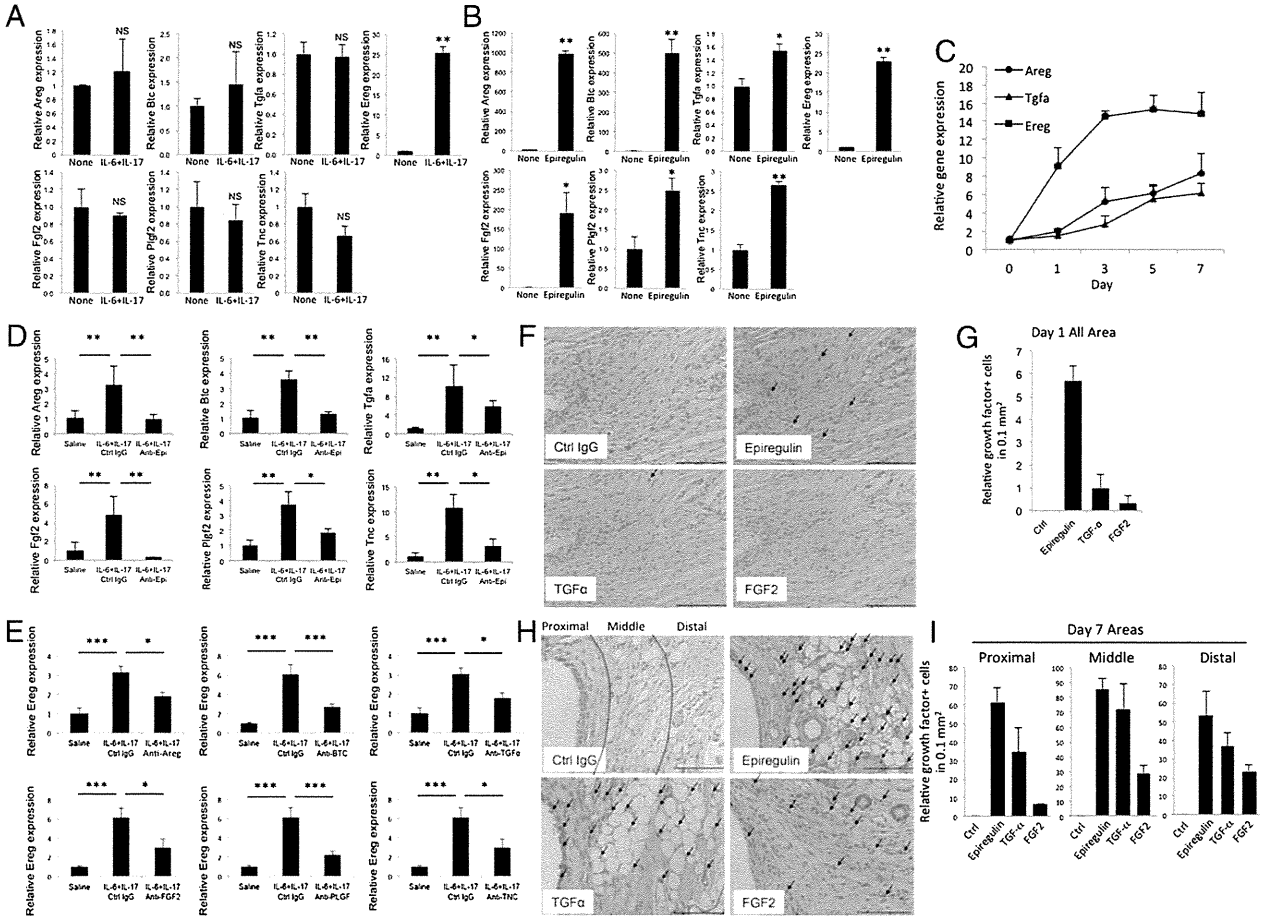

FIGURE 3. Presence of epiregulin-triggered temporal expressions in affected tissues of cytokine-induced arthritis. (**A**) mRNA expressions of Areg, Btc, Tgfa, epiregulin (Ereg), Fgf2, Plgf2, and Tnc in BC1 cells in the presence or absence of stimulation with IL-17 and IL-6 were evaluated 3 h later using real-time PCR. (**B**) mRNA expressions of Areg, Btc, Tgfa, Ereg, Fgf2, Plgf2, and Tnc in BC1 cells in the presence or absence of epiregulin stimulation were evaluated 3 h later using real-time PCR. (**C**) IL-17 (0.2 μg) and IL-6 (0.2 μg) on days 0, 1, and 2 were injected into the knee joints of F759 mice followed by analysis of expressions of Ereg, Areg, and TGF-α in joint synovial tissues on days 0, 1, 3, 5, and 7 ($n = 3$ for each condition). (**D** and **E**) IL-17 (0.2 μg) and IL-6 (0.2 μg) on days 0, 1, and 2 were injected into the knee joints of F759 mice in the presence or absence of joint injections of anti-Ereg Ab (1 μg, $n = 12$), anti-Areg Ab (1 μg, $n = 12$), anti-BTC Ab (1 μg, $n = 12$), anti–TGF-α Ab (1 μg, $n = 12$), anti-FGF2 Ab (1 μg, $n = 12$), anti-PLGF2 Ab (1 μg, $n = 12$), anti-TNC Ab (1 μg, $n = 12$), or control IgG (1 μg, $n = 12$) on days 0, 1, 2, 4, and 6 followed by analysis of the expressions of Ereg, Areg, Btc, TGF-α, FGF2, Plgf2, and Tnc (D) and Ereg (E) in joint synovial tissues on day 7. (**F–I**) IL-6 (1 μg) and IL-17 (1 μg) on days 0, 1, and 2 were injected into the left ankle joints of F759 mice followed staining by using antibodies against Ereg, TGF-α, and FGF2 in paraffin sections of left ankle joints on days 1 (F) and 7 (H) by immunohistochemistry. These experiments were performed at least three times independently; representative data are shown. Arrows indicate cells expressing growth factors in the ankle joint synovial tissues. Scale bars, 100 μm. Quantification of the histological analysis (10 × 0.1 mm^2 field) for (F) and (H) is shown (G and I). Mean scores 6 SD (A–E) and mean scores 6 SEM (G and I) are shown. The p values were calculated using a Student t test (A and B) and one-way ANOVA (D and E). $*p < 0.05$, $**p < 0.01$, $***p < 0.001$.

epiregulin, but not TGF-α or FGF2, was observed in the joints 1 d after IL-17A and IL-6 cytokine injections (Fig. 3F, 3G). The expressions of epiregulin and TGF-α were broad in the joints by day 7 after cytokine injections, whereas those of FGF2 were restricted to the middle and distal areas (Fig. 3H, 3I). Thus, growth factor expressions are regulated in an epiregulin-triggered temporal manner in the affected joints of F759 arthritis.

Growth factors are increased in patients with MS and are critical for the development of an MS model, EAE

We also investigated roles of growth factor expressions during the development of other autoimmune diseases. We found that Areg, BTC, TGF-α, FGF2, PLGF, and TNC were increased in sera of patients with MS (Fig. 4A), consistent with sera from patients suffering from MS having higher concentrations of epiregulin than sera from control subjects (4). We further investigated the growth factors in an MS model, EAE. The expressions of growth factors increased in the L5 cord where pathogenic $CD4^+$ T cells are initially accumulated (Fig. 4B), suggesting that the growth factors are involved in the development of EAE. Importantly, administrations of anti–TGF-α Ab or anti-epiregulin Ab significantly suppressed the development of EAE (Fig. 4C, Supplemental Fig. 4B). Serum IL-6 and the number of infiltrating $CD4^+$ cells with IL-17 or IFN-γ in the L5 cord were also decreased after treatment of anti–TGF-α Ab (Fig. 4D, 4E). Additionally, we constantly detected low cell numbers in the spinal cords after EAE induction where we previously reported similar numbers of T cells (4). These results support the idea that the regulation of growth factors contributes to the development of inflammation in other autoimmune diseases such as MS.

Discussion

We recently showed that the epiregulin/ErbB1 axis is involved in the development of inflammation in an RA model, an MS model, and a chronic rejection model (4, 16). In this study, we show that serum concentrations of growth factors including not only epiregulin, but also Areg, BTC, TGF-α, FGF2, PLGF, and TNC, increase in RA patients, suggesting that various growth factors are involved in RA development. Indeed, joint injections of IL-17A and IL-6, which induce arthritis in F759 mice, increased the local expression of these growth factors. At the same time, blockades of these factors suppressed the development of cytokine-induced arthritis in F759 mice. Moreover, we showed that many growth factors such as epiregulin, Areg, BTC, TGF-α, and FGF2 were increased in sera of patients suffering from MS and in the L5 cord of EAE, an MS model, and that blockade of TGF-α or epiregulin suppressed the development of EAE (Fig. 4C, Supplemental Fig. 4B). These results suggest that various growth factors might be independent therapeutic targets for various inflammatory diseases, including RA and MS.

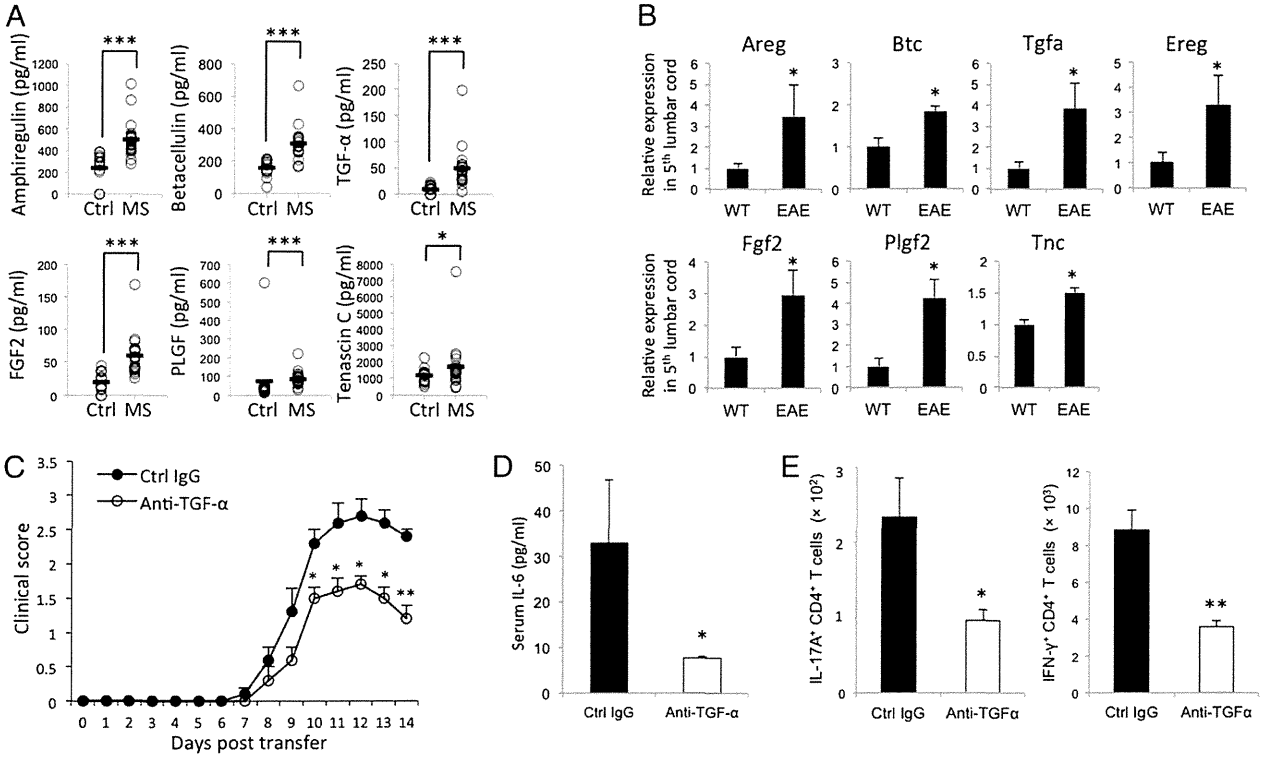

FIGURE 4. Growth factors are critical for the development of an MS model, EAE. (**A**) Serum concentrations of Areg, BTC, TGF-α, FGF2, PLGF, and TNC in patients suffering from MS ($n = 21$) compared with healthy age- and sex-matched subjects ($n = 15$). (**B**) mRNA expressions of epiregulin (Ereg), Areg, Btc, TGF-α, FGF2, Plgf2, and Tnc in the L5 cord 7 d after transfer of pathogenic $CD4^+$ T cells were evaluated using real-time PCR. (**C–E**) Pathogenic $CD4^+$ T cells isolated from EAE mice were i.v. transferred into wild-type C57BL/6 mice in the presence or absence of anti–TGF-α Ab administration (i.p., days 0–5 after the pathogenic $CD4^+$ T cell transfer). (C) Clinical EAE scores ($n = 5$ each) and (D) serum IL-6 concentrations in mice ($n = 15$). (E) Mononuclear cells from L5 spinal cords of Th17-transferred C57BL/6 mice were isolated on day 10. The resulting cell populations were counted and stimulated in vitro with MOG peptide and bone marrow–derived dendritic cells. Twenty-four hours after in vitro stimulation, intracellular IL-17 and IFN-γ levels were examined. The numbers of $CD4^+IL\text{-}17^+$ and $CD4^+IFN\text{-}\gamma^+$ T cells in spinal cords were significantly lower in recipients treated with anti–TGF-α Ab ($n = 5$) than in those treated with control IgG ($n = 5$). Individual scores, mean scores (A), and mean scores ± SEM (B–E) are shown. The p values were calculated using Wilcoxon tests (A and C) and Student t test (B, D, and E). $^*p < 0.05$, $^{**}p < 0.01$, $^{***}p < 0.001$.

We also analyzed the molecular mechanism for how these growth factors work independently to develop inflammation. We first investigated the expressions of these growth factors in affected joints during the course of the arthritis development. Only epiregulin was induced at the early phase of the inflammation, but other growth factors showed increased expression in the joints at the late phase. Furthermore, epiregulin expression itself was also dependent on the expression of each growth factor during the late phase of inflammation. Consistent with these in vivo results, in vitro experiments showed that IL-17A and IL-6 increased epiregulin expression but not other growth factors, but that epiregulin increased the expression of other growth factors. These results strongly suggest epiregulin-triggered temporal expression of growth factors in the affected tissues, which induces reciprocal regulation of the growth factors, is involved in the development of inflammation during cytokine-induced arthritis. Thus, one explanation for why growth factors work independently to develop inflammation is their temporal regulation in the affected tissues.

Interestingly, there are two kinds of growth factors that contribute to inflammation development. One group includes factors that enhance activation of the inflammation amplifier, such as epiregulin, Areg, BTC, TGF-α, and FGF2. These factors enhance activation of the inflammation amplifier via the PI3K/NF-κB pathway. The second group includes PLGF2 and TNC, which increase cell proliferation. We hypothesize that the increased cell numbers by PLGF2 and TNC enhanced the activation of the inflammation amplifier, because various growth factors and cytokines, including NF-κB and STAT3 stimulators, surround the fibroblasts to enhance proliferation. Moreover, the affected tissues in EAE contained various growth factors, including PLGF2 and TNC. Thus, we propose that a temporal expression of growth factors regulates the expression of chemokines and the proliferation of nonimmune cells, both of which contribute to inflammation in the joints of F759 mice as well as the CNS of EAE.

In summary, we investigated the relationship between growth factors and inflammation. Most growth factors tested induced IL-6 and chemokine expressions via the PI3K/NF-κB pathway. Furthermore, regional blockades of the growth factors suppressed the development of cytokine-induced arthritis. Moreover, these growth factors increased in sera of patients suffering from RA. These results suggest that each growth factor independently plays a critical role in RA development even though most of them activate similar signaling pathways. We also revealed important aspects of the molecular mechanism responsible, as epiregulin-triggered temporal regulation of the growth factors contributed to the development of inflammation, and each growth factor reciprocally regulated epiregulin in the affected tissue during the late phase of the disease development. Importantly, various growth factors increased in patients with MS and are involved in the development of EAE. We therefore conclude that these growth factors might be therapeutic targets for various inflammatory diseases, including RA and MS.

Acknowledgments

We thank Dr. Peter Karagiannis (RIKEN Quantitative Biology Center, Osaka, Japan) for carefully reading the manuscript. We also thank Dr. Seiritsu Ogura (Hosei University, Tokyo, Japan) for providing critical statistical advice.

Disclosures

The authors have no financial conflicts of interest.

References

1. Atsumi, T., R. Singh, L. Sabharwal, H. Bando, J. Meng, Y. Arima, M. Yamada, M. Harada, J. J. Jiang, D. Kamimura, et al. 2014. Inflammation amplifier, a new paradigm in cancer biology. *Cancer Res.* 74: 8–14.
2. Hirano, T. 1998. Interleukin 6 and its receptor: ten years later. *Int. Rev. Immunol.* 16: 249–284.
3. Veldhoen, M., R. J. Hocking, C. J. Atkins, R. M. Locksley, and B. Stockinger. 2006. TGFβ in the context of an inflammatory cytokine milieu supports de novo differentiation of IL-17-producing T cells. *Immunity* 24: 179–189.
4. Murakami, M., M. Harada, D. Kamimura, H. Ogura, Y. Okuyama, N. Kumai, A. Okuyama, R. Singh, J.-J. Jiang, T. Atsumi, et al. 2013. Disease-association analysis of an inflammation-related feedback loop. *Cell Reports* 3: 946–959.
5. Ogura, H., M. Murakami, Y. Okuyama, M. Tsuruoka, C. Kitabayashi, M. Kanamoto, M. Nishihara, Y. Iwakura, and T. Hirano. 2008. Interleukin-17 promotes autoimmunity by triggering a positive-feedback loop via interleukin-6 induction. *Immunity* 29: 628–636.
6. Hirano, T. 2010. Interleukin 6 in autoimmune and inflammatory diseases: a personal memoir. *Proc. Jpn. Acad. Ser. B Phys. Biol. Sci.* 86: 717–730.
7. Linardou, H., I. J. Dahabreh, D. Bafaloukos, P. Kosmidis, and S. Murray. 2009. Somatic EGFR mutations and efficacy of tyrosine kinase inhibitors in NSCLC. *Nat. Rev. Clin. Oncol.* 6: 352–366.
8. Atsumi, T., K. Ishihara, D. Kamimura, H. Ikushima, T. Ohtani, S. Hirota, H. Kobayashi, S. J. Park, Y. Saeki, Y. Kitamura, and T. Hirano. 2002. A point mutation of Tyr-759 in interleukin 6 family cytokine receptor subunit gp130 causes autoimmune arthritis. *J. Exp. Med.* 196: 979–990.
9. Sadikot, R. T., and T. S. Blackwell. 2008. Bioluminescence: imaging modality for in vitro and in vivo gene expression. *Methods Mol. Biol.* 477: 383–394.
10. Murakami, M., Y. Okuyama, H. Ogura, S. Asano, Y. Arima, M. Tsuruoka, M. Harada, M. Kanamoto, Y. Sawa, Y. Iwakura, et al. 2011. Local microbleeding facilitates IL-6- and IL-17-dependent arthritis in the absence of tissue antigen recognition by activated T cells. *J. Exp. Med.* 208: 103–114.
11. Arima, Y., M. Harada, D. Kamimura, J.-H. Park, F. Kawano, F. E. Yull, T. Kawamoto, Y. Iwakura, U. A. Betz, G. Márquez, et al. 2012. Regional neural activation defines a gateway for autoreactive T cells to cross the blood-brain barrier. *Cell* 148: 447–457.
12. Nishihara, M., H. Ogura, N. Ueda, M. Tsuruoka, C. Kitabayashi, F. Tsuji, H. Aono, K. Ishihara, E. Huseby, U. A. Betz, et al. 2007. IL-6-gp130-STAT3 in T cells directs the development of IL-17^{+} Th with a minimum effect on that of Treg in the steady state. *Int. Immunol.* 19: 695–702.
13. Ohtani, T., K. Ishihara, T. Atsumi, K. Nishida, Y. Kaneko, T. Miyata, S. Itoh, M. Narimatsu, H. Maeda, T. Fukada, et al. 2000. Dissection of signaling cascades through gp130 in vivo: reciprocal roles for STAT3- and SHP2-mediated signals in immune responses. *Immunity* 12: 95–105.
14. Sawa, S., D. Kamimura, G. H. Jin, H. Morikawa, H. Kamon, M. Nishihara, K. Ishihara, M. Murakami, and T. Hirano. 2006. Autoimmune arthritis associated with mutated interleukin (IL)-6 receptor gp130 is driven by STAT3/IL-7-dependent homeostatic proliferation of CD4^{+} T cells. *J. Exp. Med.* 203: 1459–1470.
15. Lu, Z., S. Ghosh, Z. Wang, and T. Hunter. 2003. Downregulation of caveolin-1 function by EGF leads to the loss of E-cadherin, increased transcriptional activity of β-catenin, and enhanced tumor cell invasion. *Cancer Cell* 4: 499–515.
16. Lee, J., T. Nakagiri, T. Oto, M. Harada, E. Morii, Y. Shintani, M. Inoue, Y. Takahashi, Y. Iwakura, S. Miyoshi, et al. 2012. IL-6 amplifier, NF-κB-triggered positive feedback for IL-6 signaling, in grafts is involved in allogeneic rejection responses. *J. Immunol.* 189: 1928–1936.
17. Lee, J., T. Nakagiri, D. Kamimura, M. Harada, T. Oto, Y. Susaki, Y. Shintani, M. Inoue, S. Miyoshi, E. Morii, et al. 2013. IL-6 amplifier activation in epithelial regions of bronchi after allogeneic lung transplantation. *Int. Immunol.* 25: 319–332.

World Journal of Hepatology

Submit a Manuscript: http://www.wjgnet.com/esps/
Help Desk: http://www.wjgnet.com/esps/helpdesk.aspx
DOI: 10.4254/wjh.v7.i21.2358

World J Hepatol 2015 September 28; 7(21): 2358-2362
ISSN 1948-5182 (online)

ORIGINAL ARTICLE

Retrospective Cohort Study

Development of risky varices in alcoholic cirrhosis with a well-maintained nutritional status

Hirayuki Enomoto, Yoshiyuki Sakai, Yoshinori Iwata, Ryo Takata, Nobuhiro Aizawa, Naoto Ikeda, Kunihiro Hasegawa, Chikage Nakano, Takashi Nishimura, Kazunori Yoh, Akio Ishii, Tomoyuki Takashima, Hiroki Nishikawa, Hiroko Iijima, Shuhei Nishiguchi

Hirayuki Enomoto, Yoshiyuki Sakai, Yoshinori Iwata, Ryo Takata, Nobuhiro Aizawa, Naoto Ikeda, Kunihiro Hasegawa, Chikage Nakano, Takashi Nishimura, Kazunori Yoh, Akio Ishii, Tomoyuki Takashima, Hiroki Nishikawa, Hiroko Iijima, Shuhei Nishiguchi, Division of Hepatobiliary and Pancreatic Disease, Department of Internal Medicine, Hyogo College of Medicine, Hyogo 663-8501, Japan

Author contributions: All authors participated in the studies; Enomoto H and Sakai Y wrote and edited the manuscript; all authors were involved in the manuscript revision and approved the final version of the manuscript.

Institutional review board statement: The study was reviewed and approved by Hyogo College of Medicine ethics committee.

Informed consent statement: Written informed consent about personal and medical data collection was obtained from all patients.

Conflict-of-interest statement: None of the authors have conflicts of interest to declare.

Data sharing statement: No additional data are available.

Correspondence to: Hirayuki Enomoto, MD, PhD, Division of Hepatobiliary and Pancreatic Disease, Department of Internal Medicine, Hyogo College of Medicine, 1-1 Mukogawacho, Nishinomiya, Hyogo 663-8501, Japan. enomoto@hyo-med.ac.jp
Telephone: +81-798-456472
Fax: +81-798-456474

Received: June 19, 2015
Peer-review started: June 20, 2015
First decision: July 27, 2015
Revised: August 5, 2015
Accepted: September 7, 2015
Article in press: September 8, 2015
Published online: September 28, 2015

Abstract

AIM: To compare the nutritional status between alcoholic compensated cirrhotic patients and hepatitis C virus (HCV)-related cirrhotic patients with portal hypertension.

METHODS: A total of 21 patients with compensated cirrhosis (14 with HCV-related cirrhosis and seven with alcoholic cirrhosis) who had risky esophageal varices were investigated. In addition to physical variables, including the body mass index, triceps skinfold thickness, and arm-muscle circumference, the nutritional status was also assessed using the levels of pre-albumin (pre-ALB), retinol-binding protein (RBP) and non-protein respiratory quotient (NPRQ) measured with an indirect calorimeter.

RESULTS: A general assessment for the nutritional status with physical examinations did not show a significant difference between HCV-related cirrhosis and alcoholic cirrhosis. However, the levels of pre-ALB and RBP in alcoholic compensated cirrhotic patients were significantly higher than those in HCV-related compensated cirrhotic patients. In addition, the frequency of having a normal nutritional status (NPRQ $\geqslant$ 0.85 and ALB value > 3.5 g/dL) in alcoholic compensated cirrhotic patients was significantly higher than that in HCV-related compensated cirrhotic patients.

CONCLUSION: According to our small scale study, alcoholic compensated cirrhotic patients can develop severe portal hypertension even with a relatively well-maintained liver function and nutritional status compared with HCV-related cirrhosis.

Key words: Alcoholic liver cirrhosis; Hepatitis C virus; Rapid-turnover proteins; Albumin; Nutritional status; Esophageal varices; Portal hypertension; Non-protein respiratory quotient

Core tip: We compared the nutritional status between alcoholic compensated cirrhotic patients and hepatitis C virus (HCV)-related cirrhotic compensated patients. The levels of rapid-turnover proteins in alcoholic compensated cirrhotic patients were significantly higher than those in HCV-related compensated cirrhotic patients. When the nutritional status was determined using the albumin level and non-protein respiratory quotient, the frequency of having a normal nutritional status in alcoholic compensated cirrhotic patients was significantly higher than that in HCV-related compensated cirrhotic patients. These findings suggest that alcoholic compensated cirrhotic patients can develop severe portal hypertension even with a relatively well-maintained liver function and nutritional status.

Enomoto H, Sakai Y, Iwata Y, Takata R, Aizawa N, Ikeda N, Hasegawa K, Nakano C, Nishimura T, Yoh K, Ishii A, Takashima T, Nishikawa H, Iijima H, Nishiguchi S. Development of risky varices in alcoholic cirrhosis with a well-maintained nutritional status. *World J Hepatol* 2015; 7(21): 2358-2362 Available from: URL: http://www.wjgnet.com/1948-5182/full/v7/i21/2358.htm DOI: http://dx.doi.org/10.4254/wjh.v7.i21.2358

INTRODUCTION

Chronic liver diseases (CLDs), such as hepatitis virus-related liver diseases and alcoholic liver disease (ALD), cause liver fibrosis and portal hypertension, and the development of gastroesophageal varices is a major complication in patients with advanced liver diseases[1,2]. However, ALD is suggested to have several specific mechanisms which vary from viral hepatitis-related liver diseases and contribute to the progression of liver fibrosis[3,4]. In addition, alcohol intake increases the portal vein pressure by several causes which are independent of the progression of liver fibrosis[5]. For instance, the enlargement of hepatocytes with ballooning was reported to mechanically compress the sinusoid and contribute to increased pressure of the portal vein[6-8]. Therefore, the severity of portal hypertension in alcoholic liver cirrhosis tends to be more remarkable than that in hepatitis virus-related cirrhosis, and patients with alcoholic liver cirrhosis are suggested to develop large varices even with a relatively well-maintained liver function and general clinical conditions[9-11].

Protein energy malnutrition is a major complication of cirrhotic patients, and the presence of energy malnutrition is determined by a low non-protein respiratory quotient (NPRQ) level (< 0.85) which is measured with an indirect calorimeter, and the presence of protein malnutrition was determined by a low level of serological albumin (ALB) (≤ 3.5 g/dL)[12]. Although many cirrhotic patients have nutritional problems, the differences in the nutritional status between alcoholic cirrhotic patients and hepatitis virus-related cirrhotic patients have not yet been investigated in detail.

We previously evaluated cirrhotic patients with high-risk varices and reported the importance of nutritional supporting therapy during the endoscopic treatment for gastroesophageal varices[13]. We herein performed a sub-analysis and investigated clinical variables regarding the nutritional status in compensated cirrhotic patients (Child-Pugh class A) who have portal hypertension and compared those with alcoholic cirrhosis and hepatitis C virus (HCV)-related cirrhosis.

MATERIALS AND METHODS

Of the patients enrolled in our previous study[13] (Clinical Trial Registration: UMIN000001534, https://upload.umin.ac.jp/), a total of 21 patients with compensated cirrhosis (14 with HCV-related cirrhosis and seven with alcoholic cirrhosis with Child-Pugh class A), who were admitted to our department for the treatment of esophageal varices with a high bleeding risk, were analyzed in the present study. Liver cirrhosis as the cause of portal hypertension was diagnosed according to the clinical findings, such as the laboratory data, ultrasonographic findings and endoscopic findings. The characteristics of the study population are summarized in Table 1. All clinical values were obtained on the day of the first-time endoscopic treatment for esophageal varices during hospitalization. The following physical variables were used to evaluate the nutritional status of the patients: body mass index, triceps skinfold thickness (%TSF), and arm-muscle circumference (%AMC). In addition to routine blood tests, pre-albumin (pre-ALB) and retinol-binding protein (RBP) levels were also measured as indicators which correlate the liver synthesis capacity and nutritional status.

The parameters measured by indirect calorimetry were carbon dioxide production per minute and oxygen consumption per minute[12]. The total urinary excretion of nitrogen was measured according to the methods previously reported[14]. According to the study by Tajika *et al*[12], the presence of energy malnutrition and protein malnutrition was determined as a low NPRQ level (< 0.85) and a low ALB level (≤ 3.5 g/dL), respectively. All clinical data were obtained under the fasting condition. The study was reviewed and approved by Hyogo College of Medicine Ethics Committee (Approval No. 650). Written informed consent about personal and

Table 1 Characteristics of enrolled patients with alcoholic compensated cirrhosis or hepatitis C virus-related compensated cirrhosis

Age (yr)	66.0 ± 11.5
Gender (male/female)	18/3
Child-Pugh score	5.4 ± 0.5
AST (IU/L)	43 (16-99)
ALT (IU/L)	26 (10-86)
γ-GTP (IU/L)	41 (12-821)
ALP (IU/L)	289 (191-726)
Total bilirubin (mg/dL)	1.1 ± 0.5
ALB (g/dL)	3.6 ± 0.3
Hemoglobin (g/dL)	11.4 ± 1.7
Platelet count (× 10^3/μL)	110 ± 68
Prothrombin time (%)	83.3 ± 9.1
BCAA treatment (present/absent)	9/12

Quantitative variables were expressed as the mean ± SD or median (range). BCAA: Branched-chain amino acids; AST: Aspartate aminotransferase; ALT: Alanine aminotransferases; γ-GTP: γ-glutamyl transpeptidase; ALB: Albumin; ALP: Alkaline phosphatase.

Table 2 Comparison of the general clinical characteristics between patients with alcoholic compensated cirrhosis and hepatitis C virus-related compensated cirrhosis

	Alcoholic cirrhosis (n = 7)	HCV-related cirrhosis (n = 14)	P value
Age (yr)	63.7 ± 6.8	67.2 ± 13.2	NS
Gender (male/female)	6/1	12/2	NS
Child-Pugh score	5.3 ± 0.5	5.4 ± 0.9	NS
AST (IU/L)	30 (16-99)	47.5 (27-68)	NS
ALT (IU/L)	24 (10-36)	35.5 (18-86)	NS
γ-GTP (IU/L)	113 (24-821)	29.5 (12-159)	< 0.01
ALP (IU/L)	311 (205-726)	281 (191-462)	NS
Total bilirubin (mg/dL)	1.2 ± 0.3	1.0 ± 0.3	NS
ALB (g/dL)	3.7 ± 0.3	3.6 ± 0.3	NS
Prothrombin time (%)	84.5 ± 9.6	82.7 ± 9.1	NS
Platelet (× 10^3/μL)	104 ± 51	112 ± 77	NS
BCAA treatment (+/-)	4/3	5/9	NS

BCAA: Branched-chain amino acids; NS: Not significant; HCV: Hepatitis C virus; AST: Aspartate aminotransferase; ALT: Alanine aminotransferases; γ-GTP: γ-glutamyl transpeptidase; ALB: Albumin; ALP: Alkaline phosphatase.

Table 3 Comparison of nutritional variables between patients with alcoholic compensated cirrhosis and hepatitis C virus-related compensated cirrhosis

	Alcoholic cirrhosis (n = 7)	HCV-related cirrhosis (n = 14)	P value
BMI	25.0 ± 5.8	22.7 ± 3.1	NS
%AMC	102.4 ± 2.3	105.0 ± 12.0	NS
%TSF	142.7 ± 44.3	190.5 ± 75.2	NS
REE/BMR	1.06 ± 0.13	1.02 ± 0.13	NS
FPG (mg/dL)	124 ± 56	105 ± 16	NS
IRI (μU/mL)	9.1 ± 2.6	13.8 ± 8.2	NS
HOMA-IR	2.8 ± 1.7	3.7 ± 2.5	NS
Pre-ALB (mg/dL)	16.3 ± 7.2	9.7 ± 2.7	< 0.01
RBP (mg/dL)	2.4 ± 1.3	1.4 ± 0.3	< 0.05

BMI: Body mass index; AMC: Arm-muscle circumference; TSF: Triceps skinfold thickness; REE/BMR: Resting energy expenditure/basal metabolic rate; FPG: Fasting plasma glucose; Pre-ALB: Pre-albumin; RBP: Retinol-binding protein; HCV: Hepatitis C virus; IRI: Immunoreactive insulin; HOMA-IR: Homeostasis Model Assessment for Insulin Resistance.

medical data collection was obtained from all patients.

Statistical analysis

The data between two groups were compared using Student's *t*-test (normally distributed data) or the Mann-Whitney *U* test (non-normally distributed data). The frequency of having a normal nutritional status between alcoholic compensated cirrhotic patients and HCV-related compensated cirrhotic patients were analyzed using the χ^2 test. A value of $P < 0.05$ was considered to be significant.

RESULTS

Comparison of the clinical data between patients with alcoholic compensated cirrhosis and HCV-related compensated cirrhosis

First, we compared the clinical variables between patients with alcoholic compensated cirrhosis and HCV-related compensated cirrhosis. Since all enrolled patients had a well-maintained liver function (Child-Pugh A), most of the common clinical variables (except for γ-glutamyl transpeptidase), including PT percentage, total bilirubin level, ALB level and platelet count, did not differ between the two groups (Table 2). In addition, the general assessment for nutritional status with physical examinations, such as %AMC and %TSF, did not show any significant differences between the two groups. However, when we compared the levels of pre-ALB and RBP, which are more sensitive indicators for liver synthesis capacity and nutritional status (referred to as "rapid-turnover proteins"), these protein levels were significantly higher in alcoholic compensated cirrhotic patients compared with those in HCV-related compensated cirrhotic patients, suggesting a better maintained liver condition of alcoholic compensated cirrhosis with severe portal hypertension than that of HCV-related compensated cirrhosis (Table 3).

Nutritional status in patients with compensated cirrhosis with risky varices: Comparison between alcoholic compensated cirrhosis and HCV-related compensated cirrhosis

Using the indirect calorimetry in combination with the blood test, we determined the nutritional status of each patient in detail. The frequency of having a normal nutritional status (NPRQ ⩾ 0.85 and ALB value > 3.5 g/dL) in patients with alcoholic compensated cirrhosis (5/7: 71.4%) was significantly higher than that in patients with HCV-related compensated cirrhosis (2/14: 14.2%) (Figure 1). These findings suggest that patients with alcoholic cirrhosis can develop severe portal hypertension even with a relatively well- maintained liver function and nutritional status when compared to patients with HCV-related cirrhosis.

DISCUSSION

ALD leads to an increased intrahepatic and portal

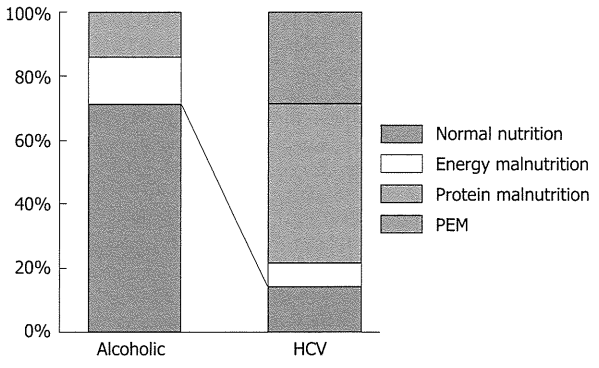

Figure 1 Nutritional status of compensated cirrhosis was determined using the albumin value and non-protein respiratory quotient. The rate of patients with a normal nutritional status (non-protein respiratory quotient level ⩾ 0.85 and albumin level > 3.5 g/dL) was significantly higher in alcoholic compensated cirrhosis than that in HCV-related compensated cirrhosis. HCV: Hepatitis C virus; PEM: Protein energy malnutrition.

pressure and portal hypertension depending on several conditions which vary from hepatitis virus-related CLDs, such as compression of the hepatic sinusoid by enlarged hepatocytes in the form of ballooning[6-8]. In addition, perivenular fibrosis, one of histological characteristics of ALD, is also suggested to contribute to the development of portal hypertension[15-17]. We herein compared several clinical parameters between Child-Pugh grade A patients with alcoholic compensated cirrhosis and those with HCV-related compensated cirrhosis. Although there were no significant differences in the general clinical variables, patients with alcoholic cirrhosis had better liver synthesis capacity and/or nutritional status. These findings suggest that alcoholic cirrhotic patients are prone to develop portal hypertension even under the condition of a well-maintained liver function and nutritional status.

In the present study, the general clinical variables including liver functional tests and physical examinations did not differ between patients with HCV-related compensated cirrhosis and alcoholic compensated cirrhosis. However, we found alcoholic compensated cirrhotic patients showed significantly higher levels of pre-ALB and RBP than HCV-related compensated cirrhotic patients (Table 2). Rapid-turnover proteins, such as pre-ALB and RBP, have shorter life-spans than ALB (pre-ALB: approximately 2 d, RBP: approximately 12 h, and ALB: approximately 3 wk). Therefore, these rapid turnover proteins are able to sensitively reflect the liver synthesis capacity and nutritional status[18-20]. In addition, in HCV-related compensated cirrhotic patients, the levels of ALB and the NPRQ were decreased in 35.7% (5/14) and 78.6% (11/14) of the patients, respectively. Although we did not clarify the role of HCV-infection in the development of malnutrition, our findings suggested that patients with HCV-related cirrhosis potentially had either protein or energy malnutrition, even compensated cirrhotic patients (Child-Pugh A) who did not exhibit cirrhosis-related clinical symptoms. It has been previously reported that cirrhotic patients with either energy malnutrition (NPRQ < 0.85) or protein malnutrition (ALB value ⩽ 3.5) have an unfavorable prognosis[12,21]. Recent advancements in antiviral treatment are expected to lead to a significant decrease in the frequency of HCV infection[22,23]. It would be interesting to evaluate changes in the nutritional status of patients with cirrhosis after the elimination of HCV-related compensated cirrhosis.

In Table 2, the mean value of %TSF was numerically higher in HCV-related cirrhotic patients than that in alcoholic cirrhotic patients, although a statistical significance was not found between the groups. Although physical examinations are generally accepted as a method to assess the nutritional status, measurement errors can easily occur (particularly regarding the levels of TSF and AMC)[13], and therefore we should pay careful attention to the evaluation of the physical variables.

Although the present study is a novel one that focused on the data of rapid-turnover proteins and indirect calorimetry in patients with compensated cirrhosis, there are some limitations associated with our study. First, the number of patients enrolled was small. It would therefore be important to investigate a larger number of patients in order to confirm our results. Second, indirect calorimetry cannot be routinely used in every institute. However, our study is unique in that it investigated compensated cirrhotic patients with similar clinical conditions (Child-Pugh grade A) and determined the differences in the nutritional parameters between patients with different etiologies. Further studies with a greater accumulation of patients and readily available tools for measuring the protein levels are necessary.

ACKNOWLEDGMENTS

We are grateful to Higuchi Y, Tawara N, Nakatani R, Kanazawa N, Matsushita Y, Fujii S, Kido H and Minemoto K (Hyogo College of Medicine) for their technical and secretarial assistance.

COMMENTS

Background

Although many cirrhotic patients have nutritional problems, the differences in the nutritional status between alcoholic cirrhotic patients and hepatitis virus-related cirrhotic patients have not yet been investigated in detail. The authors herein compared the nutritional status between alcoholic compensated cirrhosis and hepatitis C virus (HCV)-related compensated cirrhosis patients with portal hypertension.

Research frontiers

Assessment of the nutritional statuses in patients with chronic liver diseases has been increasingly important, particularly in cirrhotic patients.

Innovations and breakthroughs

This is the first report to compare the nutritional statuses between alcoholic cirrhosis and HCV-related cirrhosis patients with risky esophageal varices.

Applications

The present study showed that alcoholic compensated cirrhotic patients can develop severe portal hypertension even with a relatively well-maintained liver

function and nutritional status when compared to patients with HCV-related cirrhosis.

Peer-review

This is quite an interesting topic. It focuses on a more realistic field of knowledge.

REFERENCES

1 **Bosch J**, Groszmann RJ, Shah VH. Evolution in the understanding of the pathophysiological basis of portal hypertension: How changes in paradigm are leading to successful new treatments. *J Hepatol* 2015; **62**: S121-S130 [PMID: 25920081 DOI: 10.1016/j.jhep.2015.01.003]

2 **Garcia-Tsao G**, Lim JK. Management and treatment of patients with cirrhosis and portal hypertension: recommendations from the Department of Veterans Affairs Hepatitis C Resource Center Program and the National Hepatitis C Program. *Am J Gastroenterol* 2009; **104**: 1802-1829 [PMID: 19455106 DOI: 10.1038/ajg.2009.191]

3 **Bolognesi M**, Verardo A, Di Pascoli M. Peculiar characteristics of portal-hepatic hemodynamics of alcoholic cirrhosis. *World J Gastroenterol* 2014; **20**: 8005-8010 [PMID: 25009370 DOI: 10.3748/wjg.v20.i25.8005]

4 **Fujii H**, Kawada N. Fibrogenesis in alcoholic liver disease. *World J Gastroenterol* 2014; **20**: 8048-8054 [PMID: 25009376 DOI: 10.3748/wjg.v20.i25.8048]

5 **Luca A**, García-Pagán JC, Bosch J, Feu F, Caballería J, Groszmann RJ, Rodés J. Effects of ethanol consumption on hepatic hemodynamics in patients with alcoholic cirrhosis. *Gastroenterology* 1997; **112**: 1284-1289 [PMID: 9098014 DOI: 10.1016/S0016-5085(97)70142-2]

6 **Nakano M**, Maruyama K, Okuyama K, Takahashi H, Yokoyama K, Takagi S, Shiraki H, Ishii H. The characteristics of alcoholics with HCV infection: histopathologic comparison with alcoholics without HCV infection and chronic type C hepatitis. *Alcohol Alcohol Suppl* 1993; **1B**: 35-40 [PMID: 8003127]

7 **Blendis LM**, Orrego H, Crossley IR, Blake JE, Medline A, Isreal Y. The role of hepatocyte enlargement in hepatic pressure in cirrhotic and noncirrhotic alcoholic liver disease. *Hepatology* 1982; **2**: 539-546 [PMID: 7118067 DOI: 10.1002/hep.1840020505]

8 **Vidins EI**, Britton RS, Medline A, Blendis LM, Israel Y, Orrego H. Sinusoidal caliber in alcoholic and nonalcoholic liver disease: diagnostic and pathogenic implications. *Hepatology* 1985; **5**: 408-414 [PMID: 3997070 DOI: 10.1002/hep.1840050311]

9 **Le Moine O**, Hadengue A, Moreau R, Sogni P, Soupison T, Yang S, Hartleb M, Lebrec D. Relationship between portal pressure, esophageal varices, and variceal bleeding on the basis of the stage and cause of cirrhosis. *Scand J Gastroenterol* 1997; **32**: 731-735 [PMID: 9246716 DOI: 10.3109/00365529708996526]

10 **Momiyama K**, Nagai H, Sumino Y. Comparison of the hemodynamics between patients with alcoholic or HCV-related cirrhosis. *Hepatogastroenterology* 2011; **58**: 2036-2040 [PMID: 22234075 DOI: 10.5754/hge10121]

11 **Bolognesi M**, Sacerdoti D, Mescoli C, Bombonato G, Cillo U, Merenda R, Giacomelli L, Merkel C, Rugge M, Gatta A. Different hemodynamic patterns of alcoholic and viral endstage cirrhosis: analysis of explanted liver weight, degree of fibrosis and splanchnic Doppler parameters. *Scand J Gastroenterol* 2007; **42**: 256-262 [PMID: 17327946 DOI: 10.1080/00365520600880914]

12 **Tajika M**, Kato M, Mohri H, Miwa Y, Kato T, Ohnishi H, Moriwaki H. Prognostic value of energy metabolism in patients with viral liver cirrhosis. *Nutrition* 2002; **18**: 229-234 [PMID: 11882395 DOI: 10.1016/S0899-9007(01)00754-7]

13 **Sakai Y**, Iwata Y, Enomoto H, Saito M, Yoh K, Ishii A, Takashima T, Aizawa N, Ikeda N, Tanaka H, Iijima H, Nishiguchi S. Two randomized controlled studies comparing the nutritional benefits of branched-chain amino acid (BCAA) granules and a BCAA-enriched nutrient mixture for patients with esophageal varices after endoscopic treatment. *J Gastroenterol* 2015; **50**: 109-118 [PMID: 24633624 DOI: 10.1007/s00535-014-0950-2]

14 **Dickerson RN**, Tidwell AC, Minard G, Croce MA, Brown RO. Predicting total urinary nitrogen excretion from urinary urea nitrogen excretion in multiple-trauma patients receiving specialized nutritional support. *Nutrition* 2005; **21**: 332-338 [PMID: 15797675 DOI: 10.1016/j.nut.2004.07.005]

15 **Nakano M**, Worner TM, Lieber CS. Perivenular fibrosis in alcoholic liver injury: ultrastructure and histologic progression. *Gastroenterology* 1982; **83**: 777-785 [PMID: 7106508]

16 **Goodman ZD**, Ishak KG. Occlusive venous lesions in alcoholic liver disease. A study of 200 cases. *Gastroenterology* 1982; **83**: 786-796 [PMID: 7106509]

17 **Miyakawa H**, Iida S, Leo MA, Greenstein RJ, Zimmon DS, Lieber CS. Pathogenesis of precirrhotic portal hypertension in alcohol-fed baboons. *Gastroenterology* 1985; **88**: 143-150 [PMID: 3964762 DOI: 10.1016/S0016-5085(85)80146-3]

18 **Smith FR**, Goodman DS, Zaklama MS, Gabr MK, el-Maraghy S, Patwardhan VN. Serum vitamin A, retinol-binding protein, and prealbumin concentrations in protein-calorie malnutrition. I. A functional defect in hepatic retinol release. *Am J Clin Nutr* 1973; **26**: 973-981 [PMID: 4199432]

19 **Devoto G**, Gallo F, Marchello C, Racchi O, Garbarini R, Bonassi S, Albalustri G, Haupt E. Prealbumin serum concentrations as a useful tool in the assessment of malnutrition in hospitalized patients. *Clin Chem* 2006; **52**: 2281-2285 [PMID: 17068165 DOI: 10.1373/clinchem.2006.080366]

20 **Chaves GV**, Peres WA, Gonçalves JC, Ramalho A. Vitamin A and retinol-binding protein deficiency among chronic liver disease patients. *Nutrition* 2015; **31**: 664-668 [PMID: 25837210 DOI: 10.1016/j.nut.2014.10.016]

21 **Hanai T**, Shiraki M, Nishimura K, Imai K, Suetsugu A, Takai K, Shimizu M, Naiki T, Moriwaki H. Free fatty acid as a marker of energy malnutrition in liver cirrhosis. *Hepatol Res* 2014; **44**: 218-228 [PMID: 23601060 DOI: 10.1111/hepr.12112]

22 **Pawlotsky JM**, Feld JJ, Zeuzem S, Hoofnagle JH. From non-A, non-B hepatitis to hepatitis C virus cure. *J Hepatol* 2015; **62**: S87-S99 [PMID: 25920094 DOI: 10.1016/j.jhep.2015.02.006]

23 **van de Ven N**, Fortunak J, Simmons B, Ford N, Cooke GS, Khoo S, Hill A. Minimum target prices for production of direct-acting antivirals and associated diagnostics to combat hepatitis C virus. *Hepatology* 2015; **61**: 1174-1182 [PMID: 25482139 DOI: 10.1002/hep.27641]

P- Reviewer: He ST, Maasoumy B, Penkova-Radicheva MP
S- Editor: Tian YL **L- Editor**: A **E- Editor**: Liu SQ